Characterization of Cellulose-Nanofiber-Modified Fibrillated Lyocell Fiber Separator

Huan Song,[a,b] Jun Yang,[b] Yu Yang,[b] Qing Yang,[b] and Jian Hu [a,*]

A fibrillated lyocell fiber-based separator was prepared using lyocell fibers and was modified with cellulose nanofibers. The effects of the cellulose nanofiber addition on the tensile properties, electrical properties, pore structure, liquid absorption properties, and equivalent series resistance of the separators were studied. It was found that adding an appropriate amount of cellulose nanofibers to the fibrillated lyocell fiber separator can improve the tensile strength, elongation at break, breakdown voltage, and equivalent series resistance value of the separator; reduce the pore size and porosity of the separator; and improve the pore size distribution. Moreover, the separator modified with 4% cellulose nanofibers yielded a favorable combination of properties, with a tensile strength of 0.645 kN/m, a mean flow pore diameter of 0.771 μm, a porosity of 88.4%, a capillary rise in paper of 30.7 mm/10 min, and an equivalent series resistance value of 2.46 Ω.

DOI: 10.15376/biores.17.3.4689-4704

Keywords: Lyocell fiber; Separator; Cellulose nanofibers

*Contact information: a: State Key Laboratory of Pulp and Paper Engineering, South China University of Technology, Guangzhou 510641 China; b : ZhuZhou Times Fiber Pioneer Material Technology Co., Ltd., Zhuzhou 412000 China; *Corresponding author: ppjhu@scut.edu.cn*

INTRODUCTION

Lyocell fibers are a type of solvent-regenerated cellulose fiber with a high crystallinity, high longitudinal orientation of crystallites, and low lateral cohesion between fibrils, which allows them to be easily fibrillated under shear force, friction force, or other mechanical forces (Crawshaw and Cameron 2000). A fibrillated lyocell fiber can be manufactured into a separator for a battery and capacitor because of its high length-diameter ratio and excellent liquid absorption performance (Hwang and Lin 2002). Separators play the role in a battery or capacitor by isolating the anode and cathode materials to prevent short circuits caused by contact between the electrodes and conducting electrolyte ion circulation channel and to ensure a fast charging and discharging process. To meet the requirements for practical applications, some excellent comprehensive performance is necessary, such as, a) satisfactory isolation and insulation performance; b) high porosity, liquid absorption, and liquid retention performance; c) applicable chemical stability and inertness to avoid a reaction with the electrolytes; d) low resistance value; e) high mechanical strength and low shrinkage rate under varying thermal cycle load; and f) a smooth surface and evenly distributed pores (Jiang *et al.* 2016).

Cellulose nanofibers (CNFs) is a general term for a class of rod-like, whisk-like, and filamentous nanocellulose with one-dimensional size below 100 nm. Cellulose nanofibers not only have a high aspect ratio and large specific surface area, but they also have high strength, high crystallinity, and high hydrophilicity. They are also lightweight and a degradable and renewable biomass material, which means that they have broad application prospects in papermaking, composite materials, medicine, electronics, food, and other industrial fields (Moran *et al.* 2008; Zhang *et al.* 2017a; Zhang *et al.* 2017b).

CNF can be added to paper pulp as a retention aid. CNF is a protofibrillary fiber material with a very high specific surface area, and a large number of hydroxyl groups on the surface (Lin *et al.* 2018). After oxidation, there are a large number of carboxyl groups and groups on its surface. These characteristics make CNF easy to bind to the fiber surface with water to form a gel, even at low concentration. So when CNF is added to the slurry suspension and increases the slurry viscosity, it can be used as a natural retention aid to improve the retention rate of fine fibers and fillers. It was found that the CNF oxidized by TEMPO improved the retention of kaolin in the slurry (Guimond *et al.* 2010). In addition, the researchers also found that adding CNF obtained from TEMPO oxidation to pulp grinding calcium carbonate (GCC) caused increased retention efficiency of GCC particles in the paper (Amma-la *et al.* 2013).

In this study, the effect of various proportions of CNFs on the performance of a separator, *i.e.*, the tensile properties, electrical properties, liquid absorption, pore structure, and equivalent series resistance (ESR) value, were studied.

EXPERIMENTAL

Preparation of Fibrillated Lyocell Fibers

Lyocell fibers (4 mm, 1.7 dtex, provided by Lenzing, Austria) were dispersed into water with a concentration of 3%, and soaked for 8 h. Then, they were refined in a valley beater (S40130, Frank-PTI GmbH, Birkenau, Germany) under a pressure of 1 N·mm^{-1} until the degree of beating reached 85 °SR.

Preparation of Cellulose-Nanofiber (CNF)-Modified Separator

Cellulose nanofibers (diameter of 30 nm to 50 nm, length of 800 to 1200 nm, provided by Northern Century Cellulose Materials, Xuzhou, China) were added to a slurry of fibrillated lyocell fibers at dry-weight ratios of 0%, 0.2%, 0.4%, 0.6%, 0.8%, 1%, 2%, 3%, 4%, 5%, 6%, and 7% with respect to the lyocell fiber and then stirred with a mixer (S95568, Frank-PTI GmbH, Birkenau, Germany) for 20 min at a stirring speed of 200 rpm. Then, the CNF-modified separators were prepared using a standard sheet former (S95854, Frank-PTI GmbH, Birkenau, Germany) with a basis weight of 16 g/m^2.

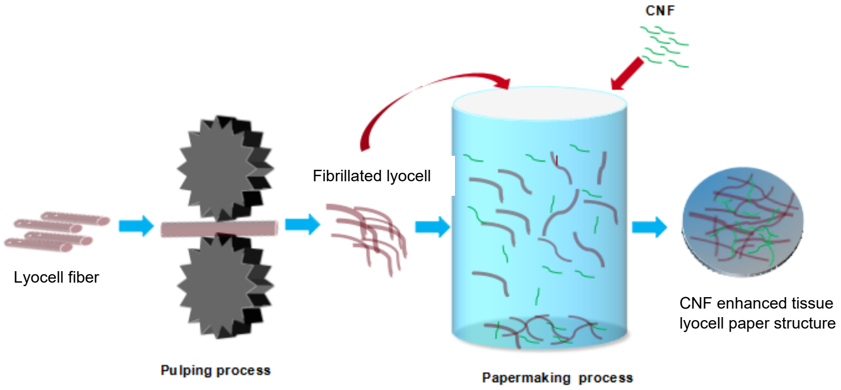

Fig. 1. Schematic of the preparation of the CNF-modified separator

Characterization

The basis weight was tested according to GB/T 451.2 (2002), the thickness and compactness were tested according to GB/T 451.3 (2002), the tensile strength and elongation at break were tested according to GB/T 12914 (2018), and the capillary rise was tested according to GB/T 461.1 (2002). In addition, the surface morphologies were observed *via* scanning electron microscope (SEM, EVO18, Carl Zeiss AG, Oberkochen, Germany), the pore size and distribution was tested *via* a PMI capillary flow aperture meter (CFP100A, PMI, Ithaca, NY), and the breakdown voltage was tested according to GB/T 3333 (1999) with a voltage boost speed of 0.1 kV/s.

The porosity of the separator was measured *via* the medium saturation method; the samples were cut into 30 mm x 30 mm pieces and soaked in ethylene glycol for at least 12 h to ensure the pores were filled. Then, by weighing the samples before and after impregnation. The porosity (ε) was calculated according to Eq. 1,

$$\varepsilon = \frac{p_{s(m_q - m_d)}}{p_e \times m_d} \tag{1}$$

where m_w and m_d are the weights of the wet and dry separator, respectively; ρ_s is the compactness of the separator; and ρ_e is the density of ethylene glycol.

To evaluate the ESR value, the samples were cut into a circular shape with a diameter of 38 mm and soaked in the electrolyte for 2 min. The samples were taken out with tweezers and held vertically for 15 to 20 s. Then, the samples were placed in a dielectric test fixture (16451B, Keysight, Santa Rosa, CA) and the ESR value was measured with an LCR meter (E4980A, Keysight, Santa Rosa, CA).

The hydrogen bond content of the cellulose fibers was analyzed *via* Origin-software-assisted FT-IR analysis. Before the test, the sample was placed in a constant temperature and humidity of 50%RH and 23 °C for 8 h, so that the moisture was about 7.4%. The FTIR absorption spectra were obtained with a Fourier-transform infrared spectrometer (JYH-127 Frontier, PerkinElmer, Waltham, MA) with scans ranging from 600 to 4000 cm^{-1}. The peak position center of each intramolecular and intermolecular hydrogen bond was determined according to the peak range of each intramolecular and intermolecular hydrogen bond in the FT-IR spectrum; then, the Gaussian fitting peak splitting method in Origin software was used to process and analyze the hydrogen bonds in the FT-IR spectrum of the sample cellulose fibers. In the fitting results, information regarding each sub-peak area, peak center wave number, and peak intensity were obtained. Then, according to the area and intensity of each sub-peak, the proportions of intramolecular hydrogen bonds and intermolecular hydrogen bonds among the total hydrogen bonds were calculated to determine the relative content of the various hydrogen bonds for quantitative analysis of the hydrogen bond mode in the cellulose fibers (Xu and Yan 2013).

RESULTS AND DISCUSSION

Characteristics of Fibrillated Lyocell Fiber Separator

Separators for batteries and capacitors should meet the following requirements: good insulation performance, high porosity, good liquid absorption performance, high mechanical strength, suitable pore size, and concentrated distribution in the appropriate size range (Shan *et al.* 2017).

Figure 2 shows the surface topography of the fibrillated lyocell fiber separator, which was found to have a rich porous structure.

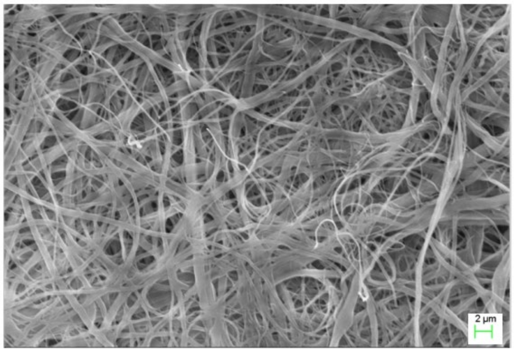

Fig. 2. SEM image of fibrillated lyocell fibers

Table 1 shows the properties of the fibrillated lyocell fiber separator. The separator had a very small thermal contraction at 200 °C, which can fully meet the requirements of the long-term operation of the capacitor and other components under 150 °C operating conditions. In addition, the separator also had good permeability, suction, and porosity, but its tensile strength and electrical breakdown performance was not high and the tensile strength was low. The separator demonstrated good liquid absorption and porosity, but its tensile strength and electrical breakdown performance were not high. If the tensile strength is too low, it will affect the smooth progress of the cutting and winding process of the battery manufacturing process. If the breakdown voltage is too low, the withstand voltage rating of the capacitor will be small, which may lead to a short circuit of the capacitor and pose a safety hazard.

Table 1. Performance of Fibrillated Lyocell Fibers Separator

Thickness (µm)	Moisture (%)	Tensile Strength (kN/m)	Elongation at Break (%)	Mid-value of Breakdown Voltage (V)
43.4	7.4	0.47	1.44	331
Pore Size (µm)	**Porosity (%)**	**Capillary Rise (mm / 10 min)**	**ESR Value (Ω)**	**Thermal shrinkage rate (%/200 °C, 40 min)**
0.895	89.7	32.3	2.39	0.50

Characteristics of CNF-Modified Fibrillated Lyocell Fiber Separator

In this paper, CNFs were used to modify the fibrillated lyocell fiber-based separator to obtain a separator material with better comprehensive properties. In addition, the effects of the CNF dosage on the tensile strength, electrical properties, liquid absorption, pore structure, and ESR value of the separator were studied.

Tensile property of CNF-modified fibrillated lyocell fiber separator

Figure 3 illustrates the tensile strength and elongation at break for samples with various CNF additions. With an increase in the CNF addition, the tensile strength and elongation at break gradually increased. When the CNF addition was 4%, the tensile strength and elongation at break increased to 0.647 kN/m and 1.81%, respectively. When the CNF addition was greater than 4%, the increase in the tensile strength of the separator tended to be minimal.

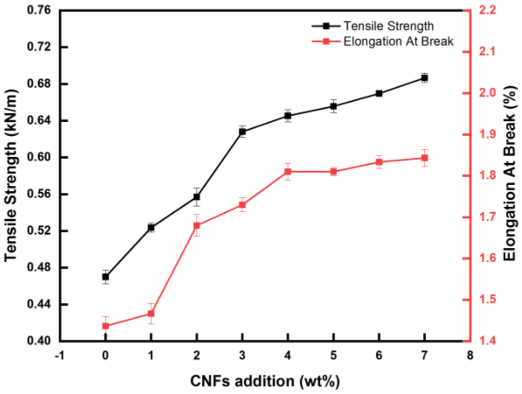

Fig. 3. Tensile strength and elongation at break curves of CNF-modified fibrillated lyocell fibers

The mechanism by which the CNF addition affects the tensile strength of the separator is discussed below, after analysis of the separator *via* scanning electron microscope and Origin-software-assisted FT-IR.

In the network cavity, the application of CNFs plays a role in enhancing the separator as follows (Siro and Plackett 2010; Boufi *et al.* 2016). The CNFs could increase the binding area of the fiber network by bridging adjacent fibers, acting as an adhesive, and thereby enhancing the strength of hydrogen bonding. Because hydrogen bonding requires the hydroxyl group distance between two fibers to be within 0.35 nm, CNFs with nano-sized lengths help to increase the bonding area by bridging adjacent fibers through the entangled network formed by nano-sized cellulose. However, the CNFs could also fill into the pores of the fiber network and increase the transmission path of the mechanical forces, thereby enhancing the mechanical strength of the separator.

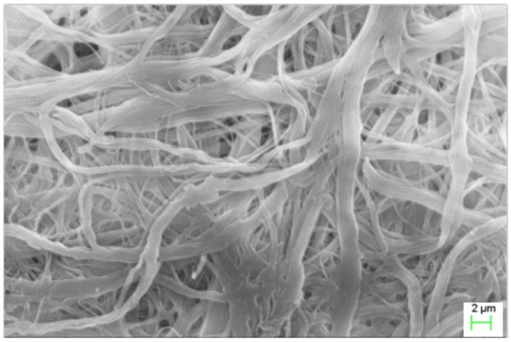

Fig. 4. SEM image of CNF-modified fibrillated lyocell fibers

The characteristic absorption wavenumbers of the intramolecular hydrogen bonds O(2)H...O(6) and O(3)H...O(5) and the intermolecular hydrogen bond O(6)H...O(3') of cellulose I are 3455 to 3410 cm^{-1}, 3375 to 3340 cm^{-1}, and 3310 to 3230 cm^{-1}, respectively (Oh *et al*. 2005). Therefore, by determining the center positions of the three characteristic absorption wave numbers of 3455 to 3410 cm^{-1}, 3375 to 3340 cm^{-1}, and 3310 to

3230 cm^{-1} in the second derivative spectrum, and the key position of intramolecular and intermolecular hydrogen can be determined. Then, the characteristic peaks of the hydrogen bonds were fitted according to the Gaussian fitting peak splitting method introduced in the experimental method. The intramolecular hydrogen bonds O(2)H...O(6) and O(3)H...O(5) and the intermolecular hydrogen bonds O(6)H...O(3') are represented by I, II, and III, respectively, in Fig. 5. According to the fitting results shown in Table 2, after adding the CNFs, the proportion of total intramolecular hydrogen bonds O(2)H...O(6) and O(3)H...O(5) among the total hydrogen bonds of cellulose fibers gradually decreased, and the proportion of the intermolecular hydrogen bond O(6)H...O(3') among the total hydrogen bonds increased.

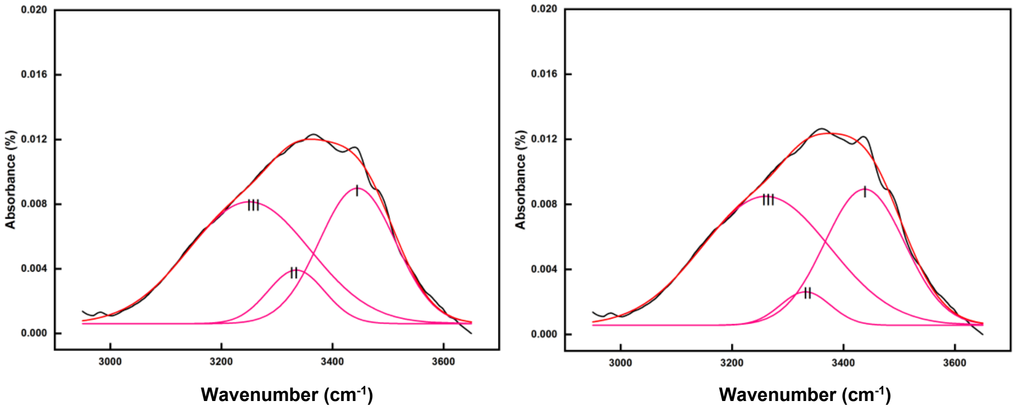

(a) 0% CNFs addition **(b)** 1% CNFs addition

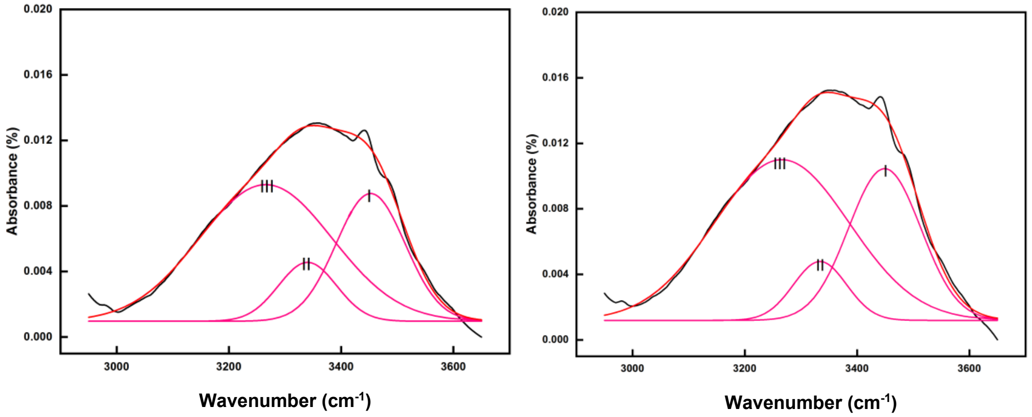

(c) 2% CNFs addition **(d)** 3% CNFs addition

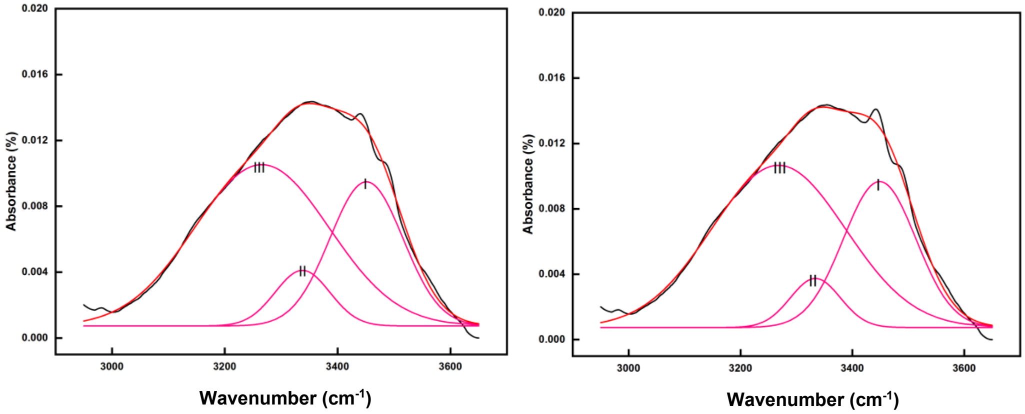

(e) 4% CNFs addition **(f)** 5% CNFs addition

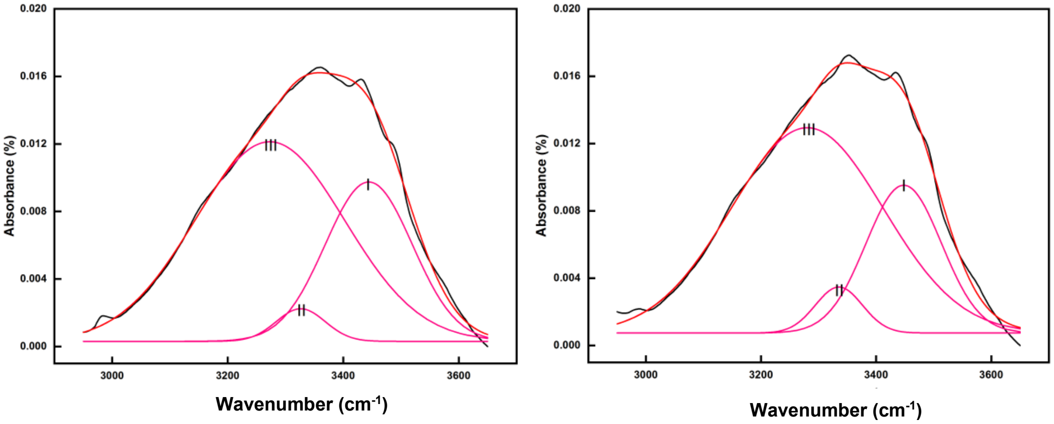

(g) 6% CNFs addition **(h)** 7% CNFs addition

Fig. 5. Analysis of the hydrogen bonds in the FT-IR spectra of the separator after adding CNFs ("I" is hydrogen bond O (2) H... O (6), "II" is hydrogen bond O (3) H... O (5); "III" is hydrogen bond O (6) H... O (3 '))

Table 2. Fitting Results for Hydrogen Bonds in the FT-IR Spectra

CNFs addition（wt%）	Peak Area	
	I and II	III
0	47.4	52.6
1.0	43.2	56.8
2.0	40.3	59.7
3.0	39.5	60.6
4.0	38.5	61.5
5.0	37.6	62.4
6.0	34.3	65.7
7.0	30.0	70.0

Figure 4 and Table 2 show that the addition of CNFs increased the bonding area of the fiber network, and more intermolecular hydrogen bonds were formed between fibers.

Therefore, the energy required to destroy the separator structure also increased, and the tensile strength increased accordingly.

Electrical properties of CNF-modified fibrillated lyocell fiber separator

Among electronic components, *e.g.* capacitors, separator materials are required to have a certain voltage resistance to improve the service life of components. Figure 6 shows the influence of the CNF addition on the electrical properties of the separator. The electric field strength of the separator considerably increased after the addition of CNFs. This is because the entanglement network formed by the CNFs and the fibrillated lyocell fiber cellulose increased the bonding area between the fibers and formed a relatively dense network structure. At the same time, some oversized holes in the diaphragm were also improved. At the same time, some oversized holes in the separator were also filled with the CNF and become smaller. Therefore the weak points that were easily broken by electric shock were greatly reduced, and the ability of the separator to withstand electric shock was considerably improved. However, with the addition of CNFs, the breakdown voltage slowly increased, which indicated that there were fewer defects in the electric breakdown film in the separator, and the electric field strength was determined primarily by the insulation characteristics of the lyocell fiber itself.

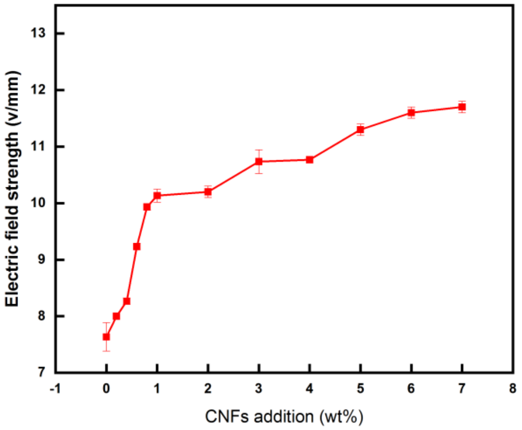

Fig. 6. Electrical properties of samples with various CNF addition

Liquid absorption of CNF-modified fibrillated lyocell fiber separator

In electronic components, *e.g.*, batteries and capacitors, the separator materials are required to have good liquid absorption, fast absorption of electrolytes, and considerable ability to absorb electrolytes, which not only can improve production efficiency, but also can prolong the life of the components. As such, the capillary liquid absorption height, as determined by the Krem method (GB/T 461.1 2002), can reflect the advantages and disadvantages of the liquid absorption performance of the separator material.

Figure 7 shows the capillary rise in paper of samples with various CNF additions. When the CNF addition was less than 4%, the capillary rise in paper slowly decreased. When the CNF addition was 4%, the capillary rise in paper decreased only slightly compared with the blank sample. However, when the CNF addition was greater than 4%, the capillary rise in paper considerably decreased, which indicates that the capillary effect of the separator was markedly weakened as a result of the increase in the density.

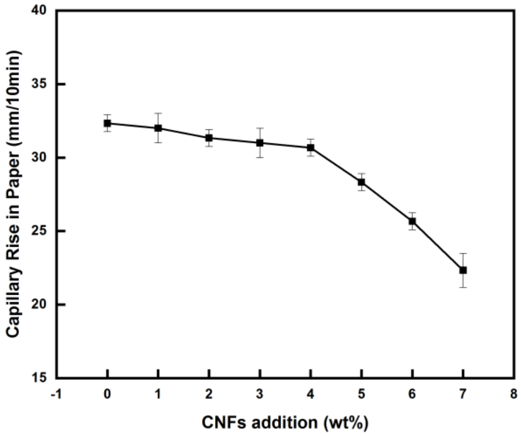

Fig. 7. Capillary rise in paper with various CNF additions

Pore structure of CNF-modified fibrillated lyocell fiber separator

The pore structure parameters of a separator generally include the pore size and porosity. The pore size and distribution affect the isolation performance and ion passing performance of the separator. If the pore size of the separator is too large, then the positively and negatively charged particles can easily pass through and cause a short circuit. If the pore size of the separator is too small, then the passing speed of the electrolyte ions will decrease and the internal resistance will increase. The porosity can reflect the microporous structure of the separator to a certain extent. The higher separator porosity allows more ions to cross the separator, but a very high porosity may weaken the puncture resistance, increase the shrinkage, and deteriorate the mechanical properties of the microporous separator, resulting in safety problems in the use of the separator.

The effects of the addition of CNFs on the pore structure of the fibrillated lyocell fibers are divided into two parts. First, CNFs with a nano-sized length were embedded into the voids formed by the fiber network, and hydrogen bonds were generated by bridging adjacent fibers. The entangled network formed by nano-sized cellulose increased the bonding area between the fibers, which improved the pore size structure and the bonding force between the reinforcing fibers. However, with an increase in the amount of CNFs added, the primary effect of the CNFs on the filling and blocking of the separator micropores became considerable. This effect is not desirable in a capacitive separator, so it is particularly important to select the appropriate amount of CNFs to be added. Figure 8 shows a schematic of the separator in terms of the effects of the addition of CNFs on the pore structure.

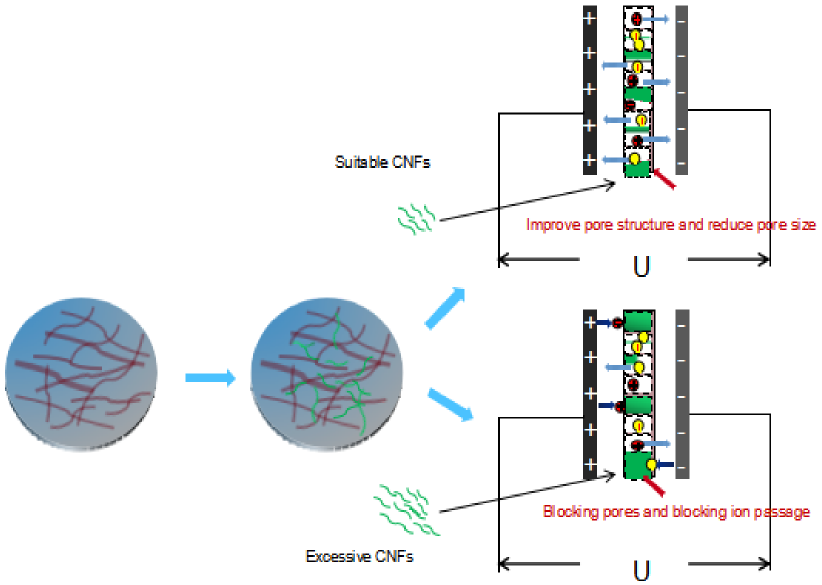

Fig. 8. Schematic of separators showing the effects of the addition of CNFs on the pore structure

The pore size and distribution of the separator are usually measured *via* a gas permeation pore size analyzer. Figure 9 shows the corresponding relationship curve between the flow and pressure obtained through dry curve, half dry curve, and wet curve tests, by which the maximum pore size, average pore size, and pore size distribution of the sample can be obtained.

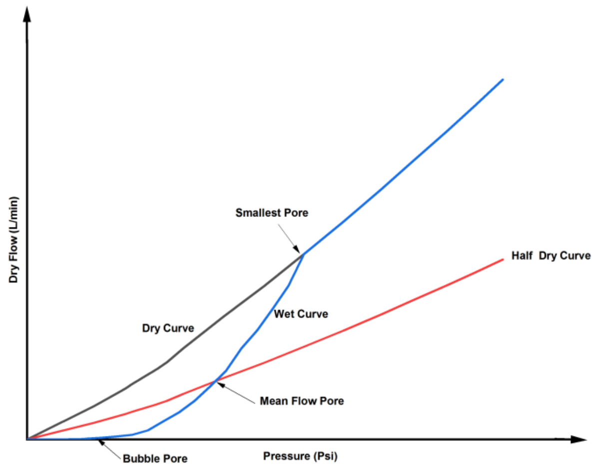

Fig. 9. Flow-pressure relationship determined from the pore tests

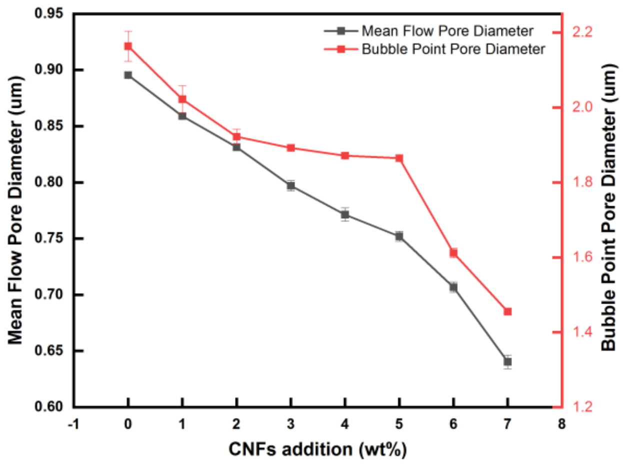

Fig. 10. Pore size of the samples with different CNF addition

Because of the different surface tensions of liquids, the tension required to determine the pore is also different. Using the American PMI capillary flow pore meter, an infiltrated sample is placed in the sample chamber, and the flow rate of the gas is controlled by the computer. When the gas inlet pressure is increased enough to overcome the capillary action between the liquid and the largest pore size, the hole is opened by the gas. The bubble point is generated through the sample, and the outlet flow rate increases significantly. The pressure difference at this time is called the bubble point pressure difference, and the corresponding pore size is the maximum pore size. As the gas pressure is further increased, new smaller holes are opened until all the holes of the sample are opened and the sample is blown dry, and the outlet flow is linear with the pressure. The pore size can be calculated according to the Washburn equation, as shown by Eq. 2,

$$D = \frac{4\gamma \cos\theta}{P} D = \frac{4\gamma \cos\theta}{P} \tag{2}$$

where D is the pore diameter, γ is the liquid surface tension, θ is the liquid contact angle, and P is the gas pressure.

In addition, the pore size distribution can be calculated according to the Washburn equation, as shown by Eq. 3,

$$f = \frac{-d[(fw/fd)\times 100]}{dD} f = \frac{-d[(fw/fd)\times 100]}{dD} \tag{3}$$

where D is the pore diameter, fw is the flow rate of the wet sample, and e is the flow rate of the dry sample.

Figures 10 and 11 show the effects of CNF addition on the pore size and distribution of the separator. When CNFs were not added, the maximum pore diameter of the separator was 2.16 µm, the average pore diameter was 0.90 µm, the pore diameter was widely distributed in the range of 0.8 to 1 µm, and the pore diameter distribution was uneven. With the addition of CNFs, the maximum pore size and average pore size of the separator decreased, and the pore size distribution range gradually narrowed. With CNF additions of 3% and 4%, the maximum pore size of the separator decreased to 1.89 µm and 1.88 µm, respectively, and the average pore size decreased to 0.80 µm and 0.77 µm, respectively.

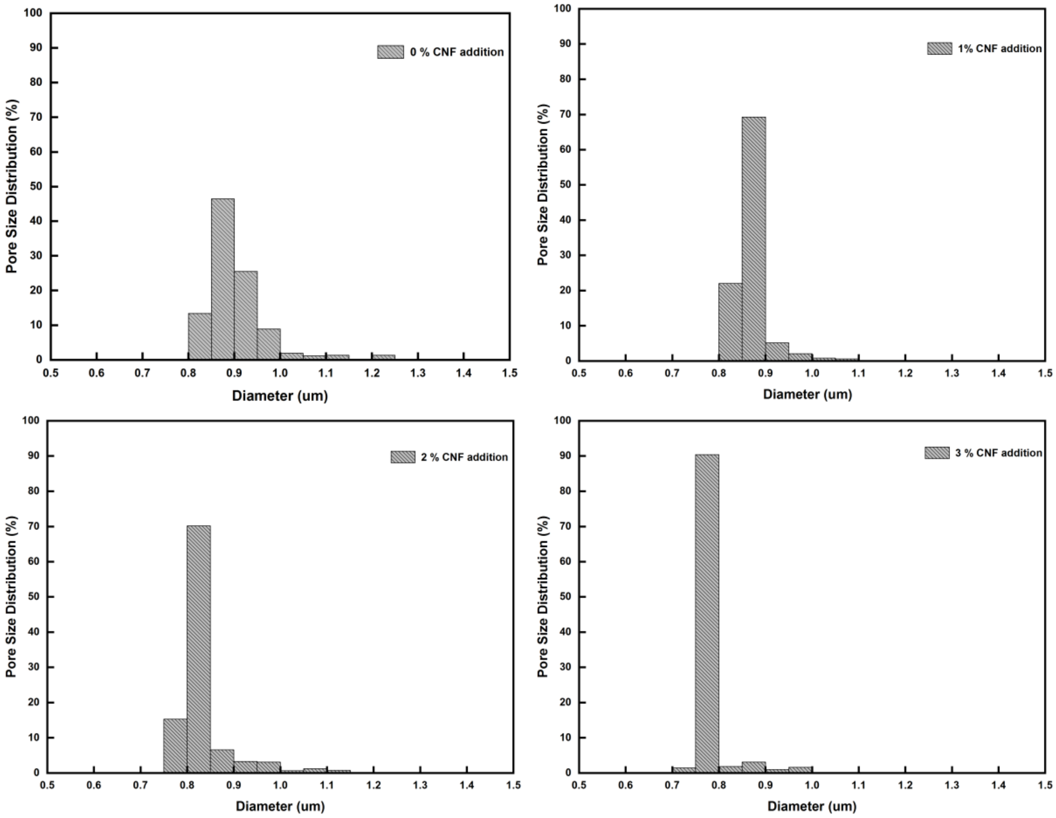

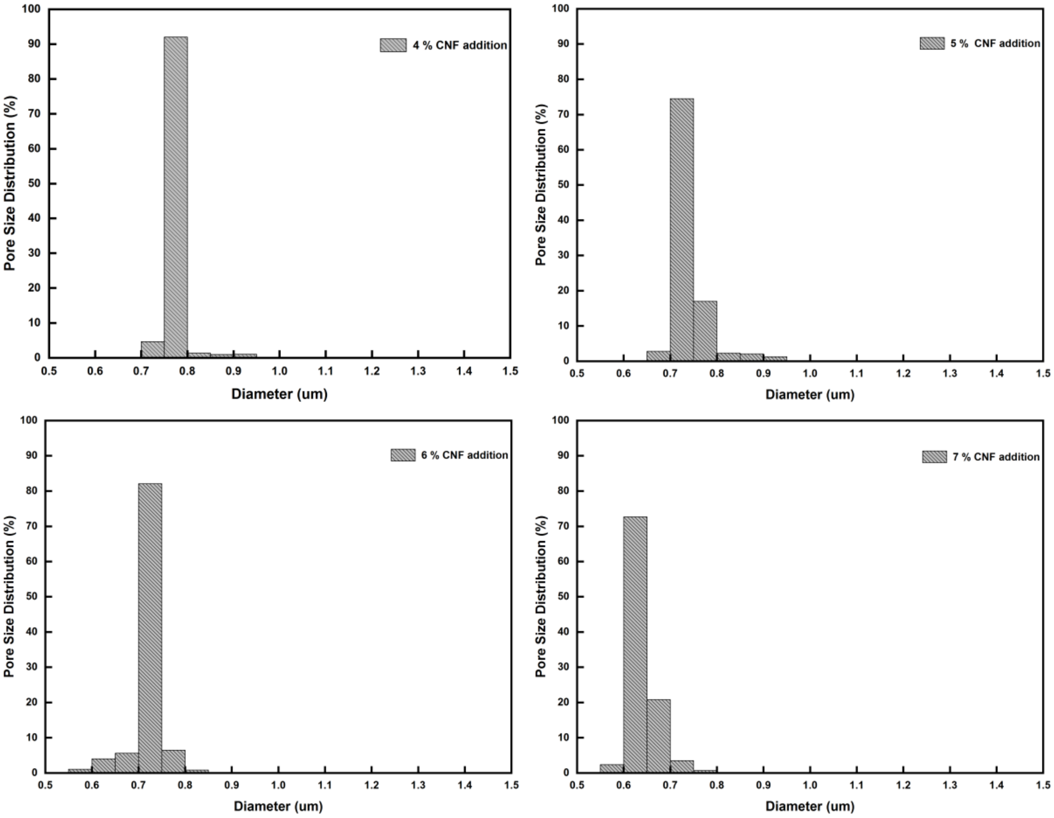

Fig. 11. Effect of different CNF addition on the pore size distribution of the separator

Greater than 90% of the pores in the separator were primarily concentrated in the diameter range of 0.75 µm to 0.8 µm, which indicates that the separator had a smaller and more uniform pore structure. With an increase in the amount of CNFs, the average pore size of the separator gradually decreased, and the concentration degree of the pore distribution gradually shifted to a smaller pore diameter. This occurred because when CNFs were added to the fibrillated lyocell membrane, CNFs with a nano-sized length were embedded between the voids formed by the fiber network and hydrogen bonds were generated by bridging adjacent fibers. The entanglement network formed by nano-sized cellulose increases the bonding area between the fibers, thus improving the pore size structure, which results in a reduction of the pore size between the fibers and a uniform distribution.

Porosity of CNF-modified fibrillated lyocell fiber separator

Figure 12 shows the effect of CNF addition on the separator porosity. When the CNF addition was less than 4%, the porosity of the separator only changed slightly, which indicates that the primary function of the CNFs was to embed into the voids formed by the fiber network and bridge the adjacent fibers. As such, they can improve the pore size structure, but the number of pores in the separator do not decrease. However, with an increase in the CNF addition, the primary effect of the CNFs on the filling and blocking of the separator micropores becomes considerable. A large number of pores are filled with the CNFs, and the porosity is considerably reduced.

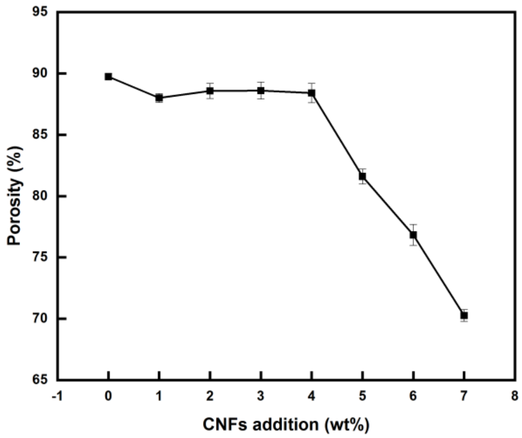

Fig. 12. Porosity of samples with various CNF addition

Equivalent series resistance value of CNF-modified fibrillated lyocell fiber separator

Theoretically, a perfect capacitor will not exhibit any energy loss; however, because of the resistance of the material of the capacitor and the loss of the insulating medium in the capacitor, the capacitor will become “imperfect” for various reasons. When a capacitor is simulated as an equivalent analog circuit, including the inductance, capacitance, and resistance, the resistance part connected in series with the capacitor is called the equivalent series resistance (ESR). The ESR will cause a voltage drop when a large capacity charging current passes through, which is very common in electronic circuits, *e.g.*, switching power supplies and frequency converters. Therefore, the stability of the output voltage is highly dependent on the ESR of the electrolytic capacitor under a large pulse current. The heat dissipation caused by the ESR can also greatly reduce the efficiency and reliability of the entire circuit system. Generally speaking, the ESR is not only an important reference factor for selecting capacitors, in addition to the capacity, withstanding voltage value, and temperature resistance value, but is also an important quality index for high-capacity electrolytic capacitors.

The ESR of a capacitor is primarily composed of the internal resistance of the electrode material, internal resistance of the electrolyte, internal resistance of the separator, and contact resistance. The internal resistance of the separator directly affects the passage of electrolyte ions and has an important impact on the reliability of a capacitor. In this experiment, the ESR value of the fibrillated lyocell fiber separator was tested using the classic physical equivalent circuit model of a capacitor, and the effect of the addition of CNFs on the ESR of the separator was studied. Figure 13 is a diagram of the experimental circuit separator used in the ESR test.

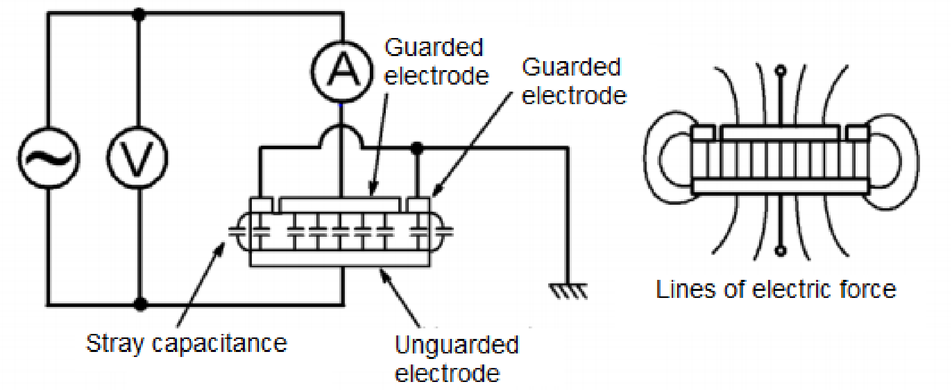

Fig. 13. Experimental circuit separator used in the ESR test

It can be seen from Fig. 14 that when the CNF addition was less than 4%, the ESR value only changed slightly, which indicates that the addition of CNFs had little impact on the ESR value. However, when the CNF addition was greater than 4%, the ESR value greatly increased. Combined with the results shown in Fig. 12, it is clear that the porosity of the separator considerably decreased, which indicates that the ion channels in the separator greatly decreased; this hinders the migration of ions, causing the internal resistance to rapidly increase.

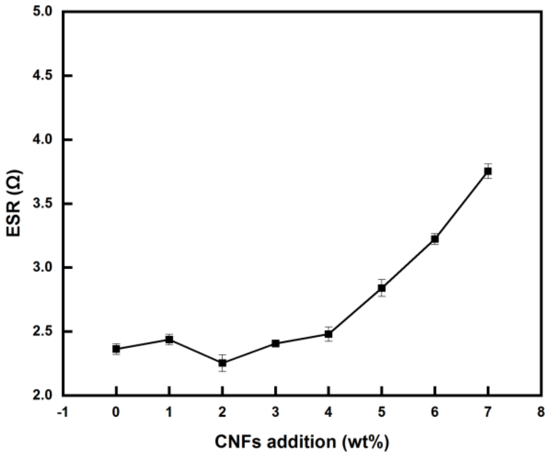

Fig. 14. ESR of samples with various CNF addition

CONCLUSIONS

1. Adding a suitable amount of cellulose nanofibers (CNFs) to a fibrillated lyocell fiber separator can effectively enhance the tensile strength, elongation at break, breakdown voltage, and other properties of a fibrillated lyocell fiber separator, as well as effectively improving the pore size of the separator.
2. Adding a suitable amount of CNFs to a fibrillated lyocell fiber separator will not have obvious adverse effects on the properties of the separator, *e.g.*, its porosity, liquid absorption height, or ESR value.

3. When the CNF addition was 4%, the comprehensive performance of the separator was the best, with a tensile strength of 0.645 kN/m, a breakdown voltage of 460.3 V, and a mean flow pore diameter of 0.771 μm. In addition, the porosity is 88.4%, the liquid absorption height was 30.7 mm/10 min, and the ESR value was 2.46 Ω.

ACKNOWLEDGMENTS

The authors are grateful for the financial support afforded by the State Key Laboratory of Pulp and Paper Engineering, and ZhuZhou Times Fiber Pioneer Material Technology Co., Ltd.

REFERENCES CITED

Ammala, A., Liimatainen, H., Burmeister, C., and Niinimaki, J. (2013). "Effect of TEMPO and periodate-chlorite oxidized nanofibrils on ground calcium carbonate flocculation and retention in sheet forming and on the physical properties of sheets," *Cellulose* 20(5), 2451-2460. DOI: 10.1007/s10570-013-0012-6

Boufi, S., González, I., Delgado-Aguilar, M., Tarrès, Q., Pèlach, M. À., and Mutjé, P. (2016). "Nanofibrillated cellulose as an additive in papermaking process: A review," *Carbohydrate Polymers* 154, 151-166. DOI: 10.1016/j.carbpol.2016.07.117

Crawshaw, J., and Cameron R. E. (2000). "A small angle X-ray scattering study of pore structure in Tencel (R) cellulose fibres and the effects of physical treatments," *Polymer* 41(12), 4691-4698. DOI: 10.1016/S0032-3861(99)00502-9

GB/T 12914 (2018). "Paper and board - Determination of tensile properties - Constant rate of elongation method (20mm/mm)," Standard. Admin. of China, Beijing, China.

GB/T 3333 (1999). "Cable paper. Determination of electrical strength at power frequency," Standardization Administration of China, Beijing, China.

GB/T 451.2 (2002). "Paper and board - Determination of grammage," Standardization Administration of China, Beijing, China.

GB/T 451.3 (2002). "Paper and board - Determination of thickness," Standardization Administration of China, Beijing, China.

GB/T 461.1 (2002). "Paper and board. Determination of capillary rise (Klemm method)," Standardization Administration of China, Beijing, China.

Guimond, R., Chabot, B., Law, K. N., and Daneault, C. (2010). "The use of cellulose nano-fibres in papermaking," *Pulp & Paper Science* 36(36), 55-61.

Hwang, K.-J., and Lin T. T. (2002). "Effect of morphology of polymeric membrane on the performance of cross-flow microfiltration," *Journal of Membrane Science* 199(1-2), 41-52. DOI: 10.1016/S0376-7388(01)00675-5

Jiang, L., Nelson, G. W., Han, S. O., Kim, H., Sim, I. N., and Foord, J. S. (2016). "Natural cellulose materials for supercapacitors," *Electrochimica Acta* 192, 251-258. DOI: 10.1016/j.electacta.2015.12.138

Lin, K.-y., An, X.-y., and Liu, H.-b. (2018). "Application of nano-cellulose in pulp and paper industry," *China Pulp & Paper* 37(1), 60-68.

Morán, J. I., Alvarez, V. A., Cyras, V. P., and Vázquez, A. (2008). "Extraction of cellulose and preparation of nanocellulose from sisal fibers.” *Cellulose* 15(1), 149-159. DOI: 10.1007/s10570-007-9145-9

Oh, S. Y., Yoo, D. I., Shin, Y., Kim, H. C., Kim, H. Y., Chung, Y. S., Park, W. H., and Youk, J. H. (2005). “Crystalline structure analysis of cellulose treated with sodium hydroxide and carbon dioxide by means of X-ray diffraction and FT-IR spectroscopy,” *Carbohydrate Research* 340(15), 2376-2391. DOI: 10.1016/j.carres.2005.08.007

Siró, I., and Plackett, D. (2010). “Microfibrillated cellulose and new nanocomposite materials: A review,” *Cellulose* 17(3), 459-494. DOI: 10.1007/s10570-010-9405-y

Shan, Hong-chen., Wang, Y., Long, Jin ., and Hu, Jian. (2017). “Influence of fibrillation of tencel fiber on absorption performance and pore size of paper,” *Paper Science & Technology* 36(1), 12-16.

Xu, Y., and Yan, Y. (2013). “Analysis on hydrogen bonding patterns of cellulose fiber by FT-IR based on origin.” *Paper and Paper Making* 32(7), 36-39.

Zhang, S., Fu, R., Dong, L., Gu, Y., and Chen, S. (2017a). “Research progress on preparation of nano cellulose and its application in composites.” *China Pulp & Paper* 36(1), 67-74.

Zhang, Z., Tao, Z., Liu Z., and Chen X. (2017b). “The research of microfibrillated cellulose and its application in paper industry: A review,” *China Pulp & Paper* 36(7), 70-78.

Article submitted: April 16, 2022; Peer review completed: June 4, 2022; Revised version received and accepted: June 16, 2022; Published: June 22, 2022.
DOI: 10.15376/biores.17.3.4689-4704